

# Microscopic mechanical properties for grain behavior of 96Mg-3Al-1Zn magnesium alloy with bending

T. SAKAI\*, J.-I. KOYAMA<sup>a</sup>

Faculty of Science and Technology, Seikei University, 3-3-1 Kichijoji-kitamachi, Musashino, Tokyo 180-8633 Japan

<sup>a</sup>AMADA Co., Ltd., 200 Ishida, Isehara, Kanagawa 259-1116 Japan

Local mechanical properties such as complex elastic modulus  $E_r$  and hardness  $H$  of a 96Mg-3Al-1Zn magnesium alloy (JIS-AZ31) were obtained by high-resolution AFM Nano-indentation complex apparatus. And surface irregularities of the grain shape were evaluated with an analytical procedure developed by applying fractal concepts and the Richardson effect. Important results of this study can be summarized as follows. (1) The fractal dimension, the SEM-EBSD analysis result, and microscopic mechanical properties are deeply related with one another. (2) The Mg alloy grain shape presents a Richardson effect. It can be expressed well quantitatively using the fractal dimension. (3) Detailed investigation of mechanical property distribution in the thickness direction revealed that complex elastic modulus distributes over about 45.0-50.0GPa, and that it is governed by the intragrain properties. (4) Microscopic mechanical properties in a single crystal grain indicate that the complex elastic modulus near grain boundaries is smaller than in the intragrain region because of the multiplication and accumulation of dislocations.

(Received May 23, 2010; accepted July 14, 2010)

**Keywords:** Magnesium alloy, SEM-EBSD analysis, Nano-indentation test, Fractal analysis, Grain behavior

## 1. Introduction

Common conventional quantitative analyses of metallic crystal grains include grain size measurement by R. L. Fullman. Recent development of an EBSD (Electron Backscattered Diffraction) orientation analysis system has enabled analysis of the crystal orientation distribution and texture. Propagation of the system has rapidly increased the amount of information related to crystal grains. However, no method has yet been established that evaluates such information and the geometric irregularity of crystal grain shape comprehensively and quantitatively. Moreover, the mechanism of microscopic shape change of crystal grains under external force has not been well elucidated.

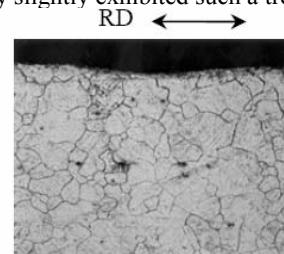
This study specifically examines a magnesium alloy that is recently attracting attention as a lightweight material; it investigates the shape change of crystal grains accompanying bending deformation in detail, and addresses its fractal property. Microscopic-scale mechanical properties of the intragrain region and grain boundary neighborhood were measured using AFM (Atomic Force Microscope) Nano-indentation complex apparatus. Grain orientation analysis was conducted using a SEM-EBSD apparatus. Then their effects on fractal properties were investigated in terms of metallography.

## 2. Specimens and crystal orientation observation of Mg alloy

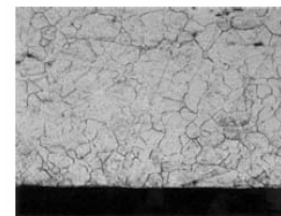
This study employed a 96Mg-3Al-1Zn Mg alloy JIS-AZ31 plate expanded to thickness  $t=1.0$  mm. It was subdivided to squares of 5.0mm $\times$ 5.0mm for the requirement of tests such as AFM and SEM-EBSD observation, and Nano-indentation. Specimens of three types were prepared; 0° (no deformation, which is as-received), 20°, and 40°, to examine the morphological change of crystal grains in the thickness direction

accompanying bending deformation. The *hcp* crystal structure of magnesium shows poor plastic deformation at room temperature. Therefore, 40° was chosen as the maximum bending angle.

Fig. 1 shows a picral-etched microstructure on the compression and tension side surface regions of a test piece after 20° bending deformation. The nominal average crystal grain size was estimated as about 40 $\mu$ m using the intercept method. Yang et al. reported a microstructure that is spherical in proportion to the bending angle on the compression side while markedly elongated to the rolling direction in the tension side, in the microstructure observation of JIS-SPCC steel. However the Mg alloy in this study only slightly exhibited such a trend.



(a) Compression side  
100  $\mu$  m



(b) Tension side

Fig. 1. Cross sectional photographs of JIS-AZ31 magnesium alloy plate.

Fig. 2 expresses the orientation map and inverse pole figure obtained from EBSD measurement result of the compression and tension side surface regions of test pieces after 0° and 40° bending deformation. The result of 0° indicates extremely wide areas expressed as a specific orientation (color), with a strong rolling texture. This suggests that only a (0001) slip system is active. At

greater than 40° bending deformation, no change is apparent in orientation distribution on the tension side surface region, although adjoining grains exhibit different colors on the compression side, indicating great orientation difference. This corresponds to different microscopic deformation behavior between the tension side and the compression side.

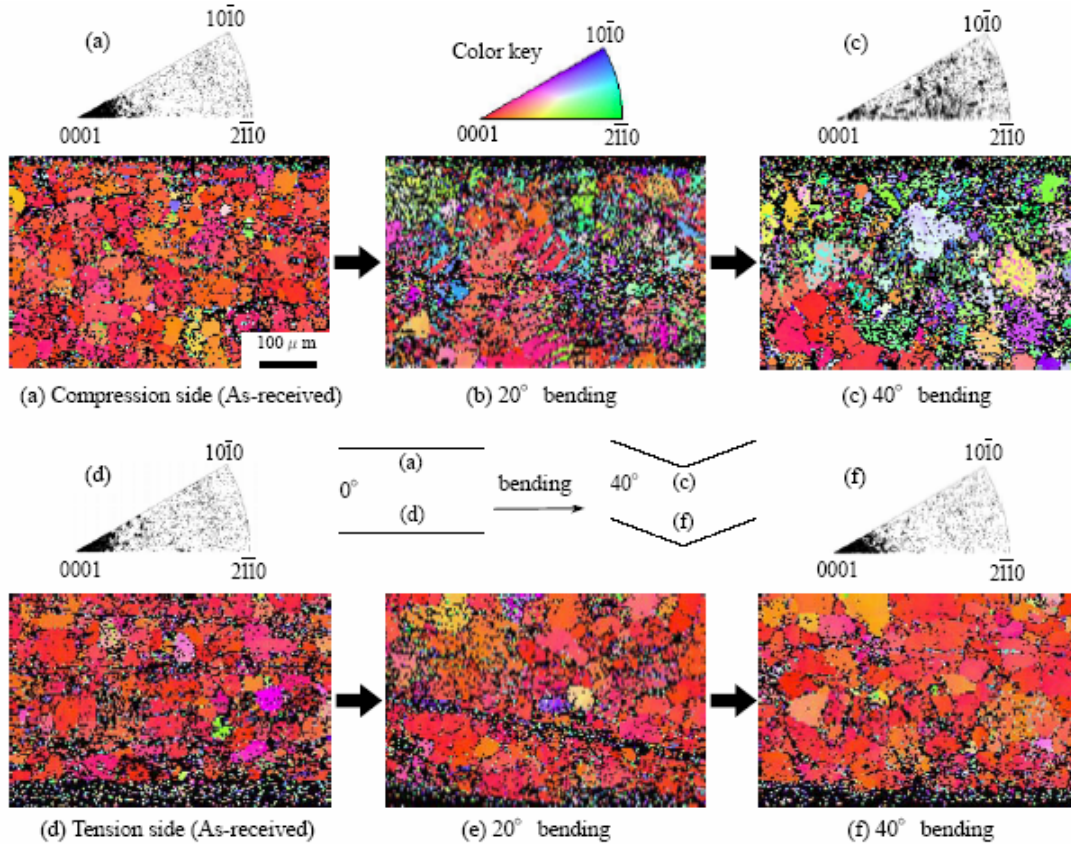


Fig. 2. Orientation imaging micrographs with color key and inverse pole figures obtained by SEM-EBSD analysis for AZ31 magnesium alloy with different bending angle.

### 3. Fractal analysis method and results

The authors have reported some results in the fields of material science and fracture mechanics on the basis of the fractal analysis method [1-4].

The principle of this analytical method lies in the Richardson effect when finding the length of a closed curve: the perimeter length varies continuously depending on the unit length of measurement. The Yardstick measurement evaluates the perimeter length of a closed curve defined by the contour of an object diagram with the line segment of a certain unit length  $\epsilon$  designated as the Yardstick. Fractal dimension  $D$  is obtained from the relation between the Yardstick number to envelop the closed curve  $n$  and the magnitude of  $\epsilon$ . Because the end point does not naturally coincide with the starting point,  $\epsilon$  varies slightly and an identical operation is repeated until the starting point and the end point meet. When the head of the last Yardstick reaches near the tail of the first

Yardstick (less than  $\epsilon/10$ ), the starting point and end point are judged to coincide in this study.

If this closed curve has a fractal nature, as L. F. Richardson confirmed for coastlines with complicated irregularity, then the following equation holds between  $n$  and  $\epsilon$ :

$$n = F\epsilon^{-D} \quad (1)$$

where  $F$  is a constant and  $D$  represents fractal dimension.  $L$ , the perimeter length of a figure approximated with a polygon of a side  $\epsilon$ , is given by the following equation:

$$L = n\epsilon = F\epsilon^{1-D} \quad (2)$$

The following equation is obtained as the logarithm of both sides of this equation.

$$\ln n\epsilon = \ln F + (1-D) \ln \epsilon \quad (3)$$

Therefore, if an irregular closed curve has fractal nature, then linearity should hold in log-log coordinates between Yardstick length  $\epsilon$  and the number of times  $n$ . Fractal dimension  $D$  is obtained from the gradient of the straight line (1- $D$ ).

An example of the  $\ln \epsilon$ - $\ln n\epsilon$  relation actually obtained from the above-described analysis method is depicted in Fig. 3 with the fractal dimension. These measurement results express the Richardson effect well. Table 1 shows that such fractal analysis was conducted continuously and that the average fractal dimension over five grains at each bending angle was acquired. A constant fractal dimension that is independent of bending angle is apparent on the tension side, although the fractal dimension decreased on the compression side. This phenomenon resembles the variation trend of crystal orientation distribution presented in Fig. 2. Thereby, it is concluded that the orientation difference brought about change in the fractal dimension.

Table 1. Numerical list of fractal dimension  $D$  of analytical results.

Analytical point	Bending angle	Fractal dimension
Compression side	0°	1.278
	20°	1.292
	40°	1.210
Tension side	0°	1.352
	20°	1.325
	40°	1.311

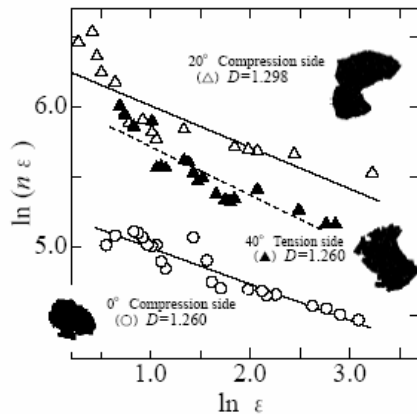


Fig. 3. Typical example of  $\ln \epsilon$  -  $\ln n\epsilon$  relationships for grain shape of AZ31 magnesium alloy.

#### 4. Evaluation of mechanical properties using the nano-indentation method

A high-resolution AFM Nano-indentation complex apparatus was used to evaluate local mechanical properties in intragrain region and grain boundary neighborhood. Complex elastic modulus  $E_r$  (including Poisson's ratio) and hardness  $H$  are derived from the initial gradient of a load-displacement curve in a loading-unloading process,

using the following relation:

$$E_r = \frac{\sqrt{\pi}}{2\sqrt{A(h_c)}} S, \quad H = \frac{P}{A(h_c)} \quad (4)$$

where  $S$  signifies the gradient of an unloading curve,  $P$  denotes penetration load, and  $A(h_c)$  represents the contact area. The indenter penetration load was set to 1,500 $\mu$ N, and the loading time to the maximum load was 10s.

Fig. 4 presents an example of the AFM image of indentation formed using a Nano-indentation test. Grains shown in the figure are at about 80 $\mu$ m depth beneath the tension-side surface region after 20° bending deformation. The test was performed on flat planes with no precipitate using the magnification shown in the figure. The figure shows that test points in the intragrain region and grain boundary neighborhood in a certain grain are denoted as IG and GB, respectively, and are marked as  $\blacktriangle$  and  $\blacktriangledown$  for distinction. Table 2 presents complex elastic modulus  $E_r$  and hardness  $H$  obtained from Nano-indentation tests. Although hardness is comparable over all specimens, the complex elastic modulus near grain boundary is lower than that of the intragrain region. The change of geometric irregular shape of grain boundaries is assumed to be attributable to the multiplication and accumulation of dislocations accompanying plastic deformation. Accordingly, the fractal dimension that directly expresses this quantitatively is related closely to local material properties. Furthermore, the mechanical property distribution of this material in the thickness direction was examined in detail at an interval of 100 $\mu$ m. The complex elastic modulus, distributed over about 45.0-50.0GPa [5], was found to be governed by intragrain properties.

Table 2. Numerical list of mechanical properties obtained by nano-indentation tests.

Point	Testing no.	$E_r$ (GPa)	$H$ (GPa)
Grain boundary (GB)	GB1	27.3	0.90
	GB2	37.4	1.06
	GB3	37.7	0.93
	GB4	38.0	0.93
Inner grain	IG1	44.5	0.83
	IG2	56.3	1.29
	IG3	46.6	0.88

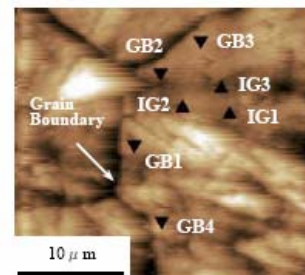


Fig. 4. AFM image after nano-indentation tests for

*tension side of cross section (after 20 °bending, depth;  
about 80 μm).*

## 5. Conclusions

(1) The fractal dimension, the SEM-EBSD analysis result, and microscopic mechanical properties obtained by Nano-indentation tests are deeply related with one another.

(2) The Mg alloy grain shape presents a Richardson effect. It can be expressed well quantitatively using the fractal dimension.

(3) Detailed investigation of mechanical property distribution in the thickness direction revealed that complex elastic modulus distributes over about 45.0-50.0 GPa, and that it is governed by the intragrain properties.

(4) Microscopic mechanical properties in a single crystal grain indicate that the complex elastic modulus near grain boundaries is smaller than in the intragrain region because of the multiplication and accumulation of dislocations.

## References

- [1] T. Sakai, T. Sakai, A. Ueno, Transactions of the Japan Society of Mechanical Engineering, Series A **64**(620), 1104 (1998).
- [2] T. Sakai, T. Sakai, A. Ueno, Transactions of the Japan Society of Mechanical Engineering, Series A **66**(644), 741 (2000).
- [3] T. Sakai, T. Sakai, A. Ueno, Transactions of the Japan Society of Mechanical Engineering, Series A **66**(652), 2183 (2000).
- [4] T. Sakai, M. Fujikawa, M. Yang, K. Manabe, Proceedings of the 8th Annual Meeting of Kanto Branch **20**(1), 247 (2002).

\*Corresponding author: sakai@st.seikei.ac.jp